Polyelectrolyte Adsorption on Charged Particles in the Debye−Hückel Approximation. A Monte Carlo Approach

Pierre Chodanowski and Serge Stoll*

Analytical and Biophysical Environmental Chemistry (CABE), Department of Inorganic, Analytical and Applied Chemistry, University of Geneva, Sciences II, 30 quai E. Ansermet, CH-1211 Geneva 4, Switzerland

Received March 16, 2000; Revised Manuscript Received January 16, 2001

ABSTRACT: Monte Carlo simulations are used to study in the Debye−Hückel approximation the complexation between a polyelectrolyte and an oppositely charged spherical particle. Attention is focused on the effect of chain length and ionic concentration on (i) the adsorption/desorption limit, (ii) the interfacial structure of the adsorbed layer, and (iii) the overcharging issue. In particular, we are interested in polyelectrolyte adsorption on particles whose surface area is small to allow the polyelectrolyte to spread to the same extent on a flat surface. The extent of polyelectrolyte adsorption is found to be the result of two competing effects: the electrostatic repulsion between the chain monomers which forces the polyelectrolyte to adopt extended conformations in solutions and limits the number of monomers which may be attached to the particle, and the electrostatic attractive interactions between the particle and the monomers forcing the chain to undergo a structural transition and collapse at the particle surface. To overcome the loss of entropy per monomer due to adsorption, it is shown that a stronger electrostatic attraction, with decreasing ionic concentration, is needed for the short chains. Below that critical ionic concentration, it is found that the degree of adsorption increases with the decrease in both the chain length and ionic strength. Trains are favored at low degrees of chain polymerization while loops are favored more when increasing the size of the chain. Above a critical chain length, electrostatic repulsions between the adsorbed monomers force the polyelectrolyte to form a protuding tail in solution. Charge inversion is also observed. Indeed, depending on the polyelectrolyte length, the number of monomers close to the particle surface is higher than it is necessary to neutralize it. Charge inversion is found to increase with the ionic concentration of the solution.

Introduction

In colloid science, aqueous solutions involving polyelectrolytes and charged particles have received a great deal of attention because of their industrial applications in the field of water treatment to promote the rate of coagulation, in food technology to control the rheology of numerous dispersions, and in powder processing to facilitate powder handling and transfer processes.[1−3] In natural waters, complexation between polysaccharide chains and mineral submicrometer particles will control the fate of trace polluants,[4] and in biology or biochemistry, a polyelectrolyte like the DNA will complex proteins.[5] In all cases the behavior of such solutions depends largely on the ability of the polyelectrolytes to adsorb and adhere to the particle surface, as well as on the structure of the adsorbed layer.

The most prominent features of polyelectrolytes, compared to nonionic polymers, are their high solubility in water and strong adsorbing capacity on surfaces bearing opposite charges. Thanks to these properties, dissolved polyelectrolytes can be used as spacers to keep surfaces apart from one another or as a polymer glue to hold the particles together.[6,7] However, in view of the complexity of adsorption processes, the applications of polyelectrolytes to real systems are often based on empirical or semiempirical observations[8−10] rather than on predictions based on theoretical[3,11−16] or computational models.[17,18] The understanding of thermodynamic as well as kinetic factors controlling the stability of colloidal dispersions of solid particles in solutions requires a knowledge of a large number of parameters such as the surface chemistry of the particles, the chemical nature (intrinsic flexibility, pK_a) and concentration of the polymer, solvent quality, pH, temperature, and ionic strength (in particular, the size and nature of the counterions). Extensive literature exists on interaction of polymers with a flat surface[3,8,9,11,13−18] and interaction between solid surfaces in the presence of polymers.[3,11,19,20] However, few studies have been reported on adsorption of supersized charged linear polymers on comparatively small oppositely charged objects. In particular, we have in mind the flocculation of submicrometer mineral particles (clays, silicates, iron and manganese oxides) by supersized extracellular polymers such as polysaccharides[4] or interactions between micelles and large polymers in aqueous solution. Using scaling concepts, adsorption of large linear neutral polymer chains on small and neutral spherical entities, so that their curvature radius is small compared to the size of the chains, has been reported by Alexander.[21] It was demonstrated that the confinement of an adsorbed chain to a finite volume is expected to lead to high excluded-volume energies which limit the molecular weight of the adsorbed part.

Experimentally, adsorption of flexible polyelectrolytes onto small micelles has been investigated by Dubin and co-workers.[22] Critical conditions for the adsorption/desorption limit have been quantitatively investigated, indicating that the critical surface charge density σ_c of micelles was proportional to the inverse Debye screening length κ. Haronska et al.[23] also examined critical conditions for the adsorption/desorption limit, focusing on polyelectrolyte charge fraction z and salt concentra-

* To whom correspondence should be addressed.

10.1021/ma000482z CCC: $20.00
Published on Web 03/02/2001

tion. Their experimental results demonstrated that κl scales as $z^{1.2}$ (where l represents the Kuhn length), close to the theoretical dependence they calculated in the limit of an asymptotically low charge fraction ($\kappa l \sim z$).

The complexation between a polyelectrolyte and an oppositely charged sphere has also been described using analytical theories. Muthukumar et al.[24] used variational methods based on a ground-state dominance approximation to predict polyelectrolyte adsorption on spherical and cylindrical surfaces. They provided an adsorption criterion and then derived the density distribution of adsorbed polyelectrolyte to determine the critical sphere radius below which adsorption does not occur. Adsorption criterion predicts that adsorption is favored when (i) lowering the temperature, chain length, and ionic concentration and with (ii) increasing the radius and surface charge density of the sphere. Netz and Joanny[25] recently provided a full complexation phase diagram for a stiff polyelectrolyte in the presence of an oppositely charged sphere. The adsorption/desorption limit was also calculated, and it was revealed that the increase of chain stiffness promotes chain desorption.

On the other hand, Monte Carlo simulations (MC) have supported some of these points. In three paper, Wallin and Linse[26−28] investigated the behavior of a polyelectrolyte−micelle complex by adjusting chain flexibility, linear charge density, and micelle radius. They focused in particular on free energy calculations to determine the key parameters influencing critical aggregation concentration. Muthukumar et al.[29] checked numerically the analytical predictions they presented in two papers.[13,24] The adsorption/desorption limits obtained by analytical theory and simulations were found to be in good agreement in the case of a planar and spherical surface by considering particle radius and salt concentration effects.

Recently, studies of the complexation of a macroion by an oppositely charged polyelectrolyte or Z ions have considered the phenomenon of overcharging. Generally speaking, this phenomenon induces charge inversion of the complex upon adsorption of multivalent ions or polyions. Mateescu et al.[30] by considering the electrostatic interaction between a spherical macroion of charge Qq and an oppositely highly charged polyelectrolyte of charge $-Nq$ demonstrate using both analytical theory and Monte Carlo simulations that for $N > Q$ the amount of collapsed polyelectrolyte on the macroion can be bigger than that required to neutralize it. They also demonstrated that overcharging increases with the diameter of the macroion until total collapse of the polyelectrolyte takes place. This phenomenon has been supported by a great deal of experimental evidence[31] by mesuring the electrophoretic mobility of the complex. For example, it has been shown[32] that negative DNA winds around a positive liposome leading to a complex called nucleosome. After an enzymatic cutting of the protuding DNA tail in solution, the complex exhibits a net negative charge that correspond to 15% overcharging. Other experiences[33] with synthetic polyelectrolytes adsorbing on planar, cylindrical, or spherical charged surfaces display a similar behavior.

Monte Carlo simulations[30,34−36] have demonstrated that on one hand overcharging increases particle diameters and on the other hand decreases with increasing chain intrinsic rigidity. Although theoretical studies agree with these facts, at this moment the origin of overcharging is not clearly defined. Park et al.[34] have proposed that counterions release, i.e., entropic effects, is the main driving force leading to overcharging. On the other hand, Mateescu et al.[30] have observed charge inversion without taking into account ions and counterions, i.e., by considering enthalpic effets only. Nguyen and Shklovskii[35] argue that overcharging comes from repulsive correlations of the multivalent ions or the polyelectrolyte turns at the macroion surface. In this manner the adsorbed Z ions or polyelectrolytes are compared to a two-dimensional strongly correlated liquid, and an analogy is made with a Wigner crystal. Adding monovalent salt makes the charge inversion stronger, exceeding in some cases 100%. Gurovitch and Sens[36] assumed that overcharging is due to connectivity between the charge of the polyelectrolyte by investigating an idealized model for the adsorption of a weakly charged polyelectrolyte.

In the present study, we use Monte Carlo simulations to investigate the complex formation between a single polyelectrolyte chain and an oppositely charged sphere. In particular, we focus on the influence of the polyelectrolyte length N. As ionic concentration C_i is expected, via screening effects, to play a key role in controlling both chain conformation and polyelectrolyte/particle interaction energy, we also focus on its influence. A simple model with an uniformly charged hard sphere to mimic a colloidal particle and a pearl necklace chain consisting of point charges connected to each other were considered in the Debye−Hückel approximation. Since a Debye−Hückel approach is used, ions and counterions are not explicitly present. The polyelectrolyte conformations are analyzed prior to and after adsorption to investigate the resulting conformational changes as well as the polymer interfacial structure, the surface coverage, and the amount of polymer adsorbed. Snapshots of equilibrated conformations are also provided. Our objective consists to give a complete description of the complex as a function of N and C_i and compare our results to some analytical predictions. In particular, we are interested in the adsorption/desorption limit dependence on N to made a comparison with Muthukumar's[24] adsorption criterion. We also investigate the overcharging issue, and comparisons are made in particular with the theoretical predictions of Nguyen's and Shklovskii's model (subsequently referred as the NS model).[35]

This paper is organized as follows. The model description and MC method are given first, and the properties of isolated polyelectrolyte chains are investigated. Then adsorption/desorption limits, polyelectrolyte conformational changes, and interfacial structures are discussed. The last part of the discussion addresses the overcharging issue. In conclusion, some possible extensions and perspectives of the present model are presented.

Model

A pearl necklace model is used to generate off-lattice 3-dimensional polymer chains. Chains are represented as a succession of N freely jointed hard spheres so as to include excluded-volume effects. Each sphere is considered to be a physical monomer of radius $\sigma_m = 3.57$ Å with a negative charge equal to -1 at its center. The fraction of ionized monomers f is set to 1 whereas the bond length is constant and equal to the Bjerrum length $l_B = 7.14$ Å. A strong polyelectrolyte chain is thus considered here at the limit of the Manning counterion condensation domain.[37]

The colloidal particle is represented as an impenetrable, uniformly charged sphere with a radius equal to $\sigma_p = 35.7$ Å. To calculate the electrostatic energy of the system, the total surface charge of the particle is assumed to be condensed into a point charge located at its center. The dielectric constant in the inner part of the particle is assumed to be the same as the surrounding medium.[38] The central point charge in the particle is kept constant with $Q = +100$, corresponding to a surface charge density of $+100$ mC m^{-2}, representative of the values observed for natural particles such as hematite at neutral pH.[39]

The solvent is treated as a dielectric medium with a relative dielectric permittivity constant ϵ_r taken as that of water at 298 K, i.e., 78.5. Thus, in this model the solvent serves only as a dielectric permittivity parameter. The total energy E_{tot} (k_BT units) for a given conformation is the sum E_{el} of the repulsive electrostatic interactions between monomers, the attractive electrostatic interactions between the chain and the particle, and the excluded-volume interactions E_{EV}

$$E_{tot} = E_{EV} + E_{el} \tag{1}$$

All pairwise interactions have been calculated without taking into account cutoff distances in our model. Hard-core repulsions between i and j lead to excluded-volume interactions using

$$E_{EV} = \sum_{i<j} u_{EV}(r_{ij}) \tag{2}$$

with

$$u_{EV}(r_{ij}) = 0 \qquad \text{when } r_{ij} > \sigma_i + \sigma_j$$
$$u_{EV}(r_{ij}) = \infty \qquad \text{when } r_{ij} \le \sigma_i + \sigma_j \tag{3}$$

where σ_i represents the radius of unit i (which can be the monomer or the particle) and $\boldsymbol{r_{ij}}$ is the distance between the centers of the two units.

All pairs of charged monomers within the polyelectrolyte interact with each other via a screened Debye–Hückel potential,

$$u_{el}(r_{ij}) = \frac{z_i z_j e^2}{4\pi\epsilon_r\epsilon_0 r_{ij}} \exp(-\kappa r_{ij}) \tag{4}$$

where e is the elementary charge ($e = 1.6 \times 10^{-19}$ C), ϵ_0 is the dielectric permittivity of the vacuum ($\epsilon_0 = 8.854 \times 10^{-12}$ C V^{-1} m^{-1}), and z_i the amount of charge on unit i.

Monomers interact with the particle according to a Verwey–Overbeek potential,

$$u'_{el}(r_{ij}) = \frac{z_i z_j e^2}{4\pi\epsilon_r\epsilon_0 r_{ij}} \frac{\exp(-\kappa(r_{ij} - \sigma_p))}{1 + \kappa\sigma_p} \tag{5}$$

Free ions are not included explicitly in the simulation; nevertheless, their overall effect on chain conformation and the monomer–particle strength of adsorption is described via the dependency of the inverse Debye screening length κ^2 [m^{-2}] on the electrolyte concentration according to

$$\kappa^2 = 1000e^2 N_A \sum_i \frac{z_i^2 C_i}{\epsilon_0\epsilon_r k_B T} \tag{6}$$

where N_A represents Avogadro's number (6.022×10^{23} [mol^{-1}]), C_i the ionic concentration [mol L^{-1}], k_B the Boltzmann constant (1.3807×10^{-23} [J mol^{-1} K^{-1}]), and T the temperature. Considering the polyelectrolyte chain at infinite dilution, the summation term includes only the species of added electrolyte and does not include polymer charges or explicit counterion effects.

A more detailed model, which is beyond the limit of this preliminary study, would require a more realistic surface–polyelectrolyte potential based on the Gouy–Chapman theory or a Coulomb potential including explicit counterions and/or solvent molecules so that local electrostatic effects could be fully effective. Inclusion of these effects using molecular dynamics or advanced Monte Carlo methods makes the model more complicated and CPU time intensive and is beyond the scope of this paper.

The Monte Carlo Method

Monte Carlo simulations were performed according to the Metropolis algorithm[40] in the canonical ensemble. In this method successive "trial" chain configurations are generated to obtain a reasonable sampling of low-energy conformations. The central monomer of the polyelectrolyte chain is placed initially at the center of a large three-dimensional spherical reflecting box of radius $2N\sigma_m$, and the particle is randomly placed in the cell. The chain and the particle are then allowed to undergo elementary movements, and after each calculation step, the coordinates of both the particle and the monomers are translated in order to replace the central monomer in the middle of the box. After each elementary random movement, the Metropolis selection criterion is employed to either select or reject the move. If the change in energy ΔE_{tot} resulting from the movement is negative, the move is selected. If ΔE_{tot} is positive, the Boltzmann factor p,

$$p = \exp\left[\frac{-\Delta E_{tot}}{k_B T}\right] \tag{7}$$

is computed and a random number $rand$ with $0 \le rand \le 1$ is generated. If $rand \le p$, the movement is selected. When $rand > p$, the trial configuration is rejected, and the previous configuration is retained and considered as a "new" state in calculating ensemble averages. This is the conformation that is perturbed in the next step. The perturbation process is continued for a given number of cycles; a typical run requires several million perturbations to equilibrate and minimize the energy of the particle–chain system. To generate new chain conformations, the monomer positions are randomly modified by elementary movements. They include three "internal" or elementary movements (end-bond, kink-jump, and crankshaft), the reptation, and the pivot. The execution of all these movements is very important to ensure the ergodicity of the calculations as well as good convergence to equilibrated conformations. It should be noted that the chain may diffuse further away and leave the particle surface during a simulation run. After relaxing the initial conformation through 10^6 cycles (equilibration period), chain properties are calculated and recorded every 1000 cycles. However, despite the

use of refined algorithms, these calculations require intensive computer processor speeds and memory capacities due to the need to investigate a large number of situations with regard to the investigation of both N and C_i effects. In our case, the application of this method currently limits the chain length to 200 monomer units.

Calculated Properties

The following definitions are used to characterize polyelectrolyte conformations and monomer positions relative to the surface of the particle. Chain properties are considered every 1000 cycles, and ensemble averages (denoted by $\langle\ \rangle$) are calculated after a period of equilibration. The mean-square radius of gyration $\langle R_g^2 \rangle$ is calculated according to

$$\langle R_g^2 \rangle = \frac{1}{N}\sum_i^N \langle (r_{cm} - r_i)^2 \rangle \tag{8}$$

where r_{cm} is the position of the mass center of the chain and r_i that of monomer i, whereas the mean-square end-to-end distance $\langle R_{ee}^2 \rangle$ is calculated as

$$\langle R_{ee}^2 \rangle = \langle (r_1 - r_N)^2 \rangle \tag{9}$$

where r_1 represents the position of the first monomer and r_N the position of the last monomer. To determine the position of the chain monomers along the coordinate normal to the surface, spherical layers around the surface are defined. The thickness of each layer is set to one monomer radius. It should be noted that the thickness of the first layer is increased to one monomer diameter to avoid any excluded-volume effect artifacts between the monomers and the particle surface. (An adjacent layer of one monomer radius in thickness is never visited by the center of the monomers.) To characterize the conformation of adsorbed chains, the mononer fraction in tails, loops, and trains is considered. The terms refer to the different conformations that are present on the surface: a train is composed of contiguous monomers that lie in the first layer, a loop lies between two trains and extends away from the surface, and a tail rises up into the solution and does not return to the surface.

Two parameters, the particle surface coverage θ and the adsorbed amount of polyelectrolyte Γ, are used to characterize the particle surface with regard to the number of monomers in the first layer. Surface coverage is defined as the fraction of the particle surface covered with the monomers which are present in the first layer,

$$\theta = \frac{a_0 N^*}{a_{surf}} \tag{10}$$

Here a_0 represents the projected area of one monomer, N^* the number of adsorbed monomers lying in the first layer, and a_{surf} the surface of the particle. The adsorbed amount Γ or the average bound fraction of the polymer chains adsorbed on the surface is defined as

$$\Gamma = \theta/\theta_{max} \tag{11}$$

where $\theta_{max} = Na_0/a_{surf}$ is the maximum fraction of the particle surface area which could be covered by a completely adsorbed polymer chain.

Results and Discussion

Chain structural changes upon adsorption are discussed by first considering isolated polyelectrolyte chains.

Table 1. Monte Carlo Equilibrated Conformations of Isolated Polyelectrolyte Chains as a Function of the Chain Monomer Number N and Ionic Concentration C_i

C_i [M] / N	0	0.001	0.01	0.1	1
25					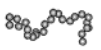
50					
100			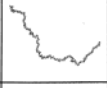		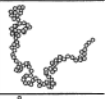
140					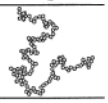
160					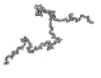
200	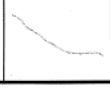				

Electrolyte concentration ranges from $C_i = 0$ M ($\kappa^{-1} = \infty$), $C_i = 0.001$ M ($\kappa^{-1} = 96$ Å), $C_i = 0.01$ M ($\kappa^{-1} = 30$ Å), $C_i = 0.1$ M ($\kappa^{-1} = 9.6$ Å) to $C_i = 1$ M ($\kappa^{-1} = 3$ Å) whereas chain lengths are adjusted to $N = 25$, 50, 100, 140, 160, and 200 monomers.

Configurational Properties of Isolated Polyelectrolyte Chains. Polyelectrolyte conformations are linked to the intensity of the electrostatic repulsions between the monomers. Nonetheless, in addition to screening effect due to added salt, the total length of the chain is also expected to play an important role because low ionic concentrations and high degrees of polymerization cause an increase of the repulsions between the monomers. Hence, by decreasing the ionic concentration, rodlike structures are favored in order to minimize the energy of the chain. It should be noted that "rodlike" does not mean a straight pole but rather an object highly oriented. When Coulombic screening increases, polyelectrolytes become less stretched; if the Debye screening length κ^{-1} is less than the distance between two charges, the polymer recovers the self-avoiding walk limit. To achieve a qualitative picture of chain conformations, equilibrated structures have been extracted from MC calculation runs and presented as three-dimensional projections in Table 1 vs C_i and N.

Scaling concepts can be applied to polyelectrolytes and the scaling exponent theoretically varies from $\nu = {}^3/_5$ (SAW limit) to $\nu = 1$ (rodlike limit) when the following relationship is considered

$$\langle R_g^2 \rangle \sim N^{2\nu} \tag{12}$$

This relationship was used to check our model hypothesis as well as the validity of our algorithms. As shown in Figure 1, the self-avoiding walk and rigid-rod models are recovered. The ratio $r = \langle R_{ee}^2 \rangle / \langle R_g^2 \rangle$, which provides a more quantitative description of chain extension, has also been investigated. For example, a random walk is identified by a value of $r = 6$, and a fully stretch polymer is characterized by $r = 12$. When a SAW chain is

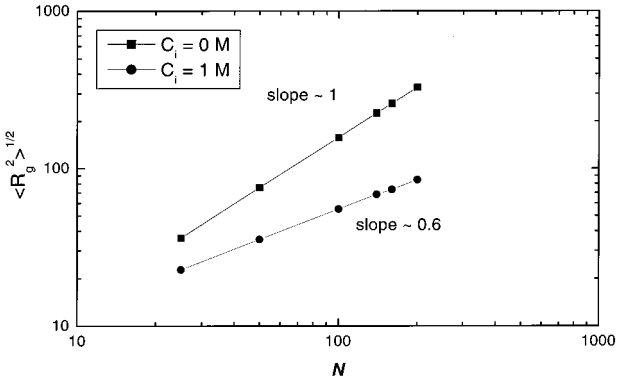

Figure 1. Root-mean-square radius of gyration $\langle R_g^2\rangle^{1/2}$ as a function of N when $C_i = 0$ and 1 M. The rigid rod and self-avoiding walk limit are observed.

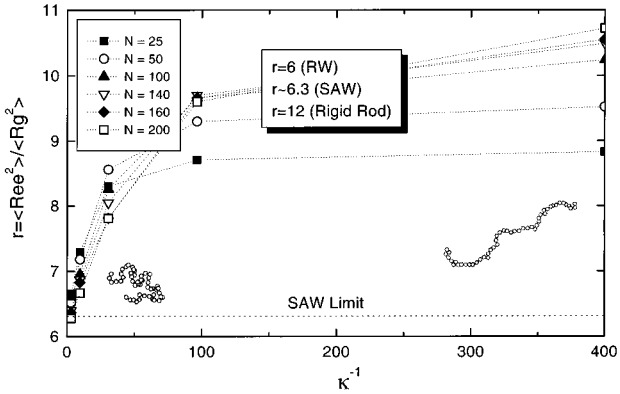

Figure 2. $r = \langle R_{ee}^2\rangle/\langle R_g^2\rangle$ as a function of κ^{-1} at various chain lengths. Fully stretched conformations are never reached. Data on the *y*-axis are for the salt-free case.

considered, r is close to 6.3. The effects of κ^{-1} and N on r are presented in Figure 2; r increases with κ^{-1} and reaches a plateau value when $\kappa^{-1} > R_{ee}$. Whatever the ionic concentration, polyelectrolytes never reach the limit $r = 12$. This is due to the fact that thermal energy always causes movements and in turn local chain deformations. When κ^{-1} is less than the distance of separation between charges along the chain backbone, r converges to 6.3 with the increase of the chain length.[41] Short chains have the largest deviation from the ideal value of r which is expected to be more representative of chains with infinite sizes. Subsequently, short chains are less stretched in the salt-free case and more swollen than the long chains in the SAW region. Thus, due to finite size effects, the curves cross each other for different values of N.

Polyelectrolyte Adsorption. To investigate adsorption processes in the polyelectrolyte/particle system, a spherical charged particle is added to the equilibrated polyelectrolyte chain so that they are close with each other. Then the polyelectrolyte/particle complex is enclosed in a spherical cell and allowed to relax. The ratio of the mean end-to-end distance of equilibrated chains in solution to the particle radius $\langle R_{ee}\rangle/\sigma_p$ vs C_i is given in Table 2 to achieve a quantitative picture of the polyelectrolyte/particle relative sizes whereas equilibrated conformations of the complex as a function of C_i and N are presented in Table 3 to achieve a more qualitative picture of the equilibrated structures. It should be noted that the extended polymer chain conformations appear smaller than their actual size as they have been reduced in size. It can be clearly seen from Table 3 that no adsorption is observed when $C_i \geq$ 1 M. Attractive surface−polymer interactions in this domain are not strong enough to overcome the entropy loss of the polymer due to its confinement near the particle. To determine the adsorption/desorption limit (a chain is considered as adsorbed when it is in contact with the particle during for more than 50% of the simulation time), the ionic concentration is adjusted between 0.3 and 1 M for each chain length. The plot of the critical ionic concentration C_i^C (ionic strength at the adsorption/desorption limit) as a function of N is presented in Figure 3. To overcome the entropy loss per monomer due to adsorption, it is demonstrated that stronger electrostatic attractions, with decreasing the ionic concentration, are needed to adsorb short polyelectrolyte chains. C_i^C increases with N from 0.34 M when $N = 25$ to 0.4 M when $N = 200$. When chains longer than 100 monomers are considered, C_i^C increases slowly to reach a plateau value close to 0.4 M. The critical electrostatic energy E_s^c associated with this limit for a single monomer in contact with the particle surface is plotted as a function of N in the inset of Figure 3. E_s^c values range from $-1.18\ k_BT$ when $N = 25$ to $-1.03\ k_BT$ when $N = 200$. Hence, adsorption is achieved when the attractive energy is greater than the thermal energy, i.e., $1\ k_BT$. These results are in accordance with the picture of polymer adsorption on flat surfaces. Indeed, in dilute solutions of polydisperse polymers, long chains are found preferentially on the surface because

Table 2. $\langle R_{ee}\rangle/\sigma_p$: Ratio of the Mean End-to-End Distance $\langle R_{ee}\rangle$ of Equilibrated Chains in Solution to the Particle Radius (σ_p = 35.7 Å) vs N and C_i

	C_i [M]				
N	0	10^{-3}	10^{-2}	10^{-1}	1
25	3.0	2.9	2.7	2.1	1.6
50	6.6	6.2	5.1	3.4	2.5
100	14.1	12.4	9.0	5.5	3.9
140	20.5	17.2	11.6	6.8	4.9
160	23.7	19.6	12.9	7.5	5.2
200	30.1	23.8	15.0	8.4	6.0

Table 3. Equilibrated Conformations of the Polyelectrolyte/Particle Complex as a Function of N and C_i

C_i [M] / N	0	0.01	0.1	0.3	1
25	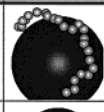	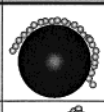	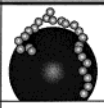	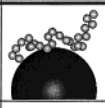	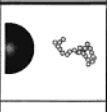
50	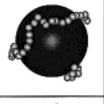	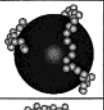	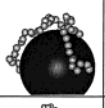	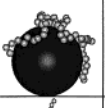	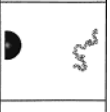
100	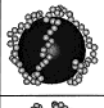	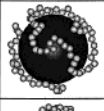	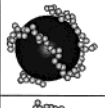	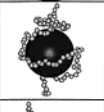	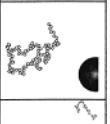
140	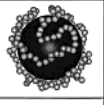	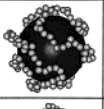	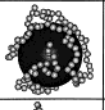	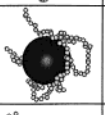	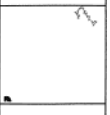
160		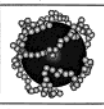	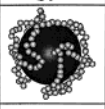	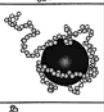	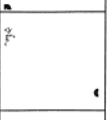
200	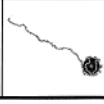	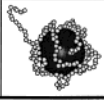	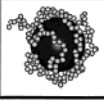	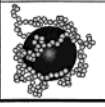	

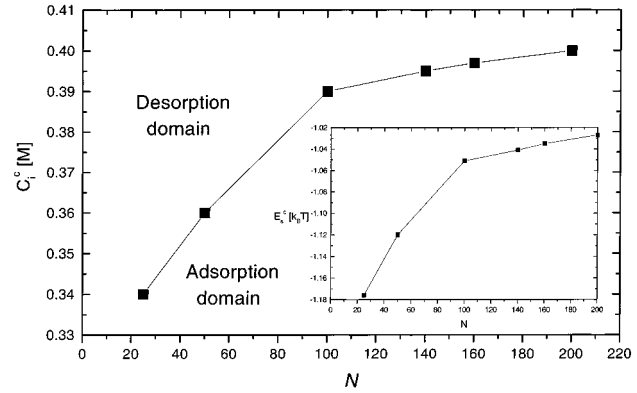

Figure 3. Adsorption/desorption limit is expressed by the variations of the critical ionic concentration C_ic as a function of N. The critical interaction energy between one monomer in contact with the particle is plotted in the inset.

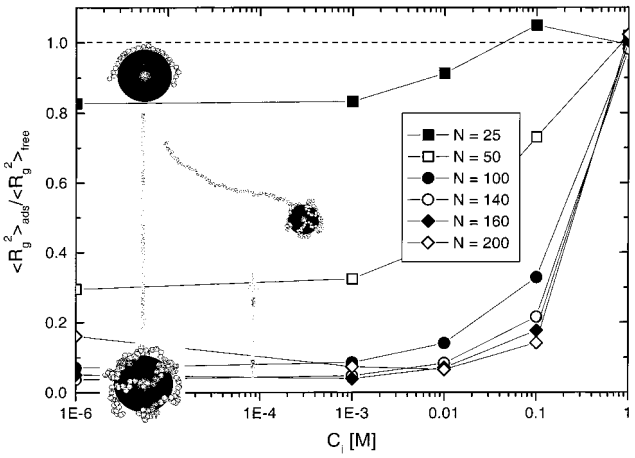

Figure 4. Ratio of the adsorbed to free chain mean-square radius of gyration as a function of C_i. Chain exhibit a maximum of deformation when $N = 140$ and $C_i = 0$ M. Data with the coordinates $\log(C_i) = -6$ correspond to the salt-free case.

less translational entropy (per unit of mass) is lost compared to the short ones, while they gain approximately the same (total) adsorption energy, even if the adsorption energy per segment is the same.[11] Such a behavior is not in agreement with Muthukumar's[24] adsorption criterion of a polyelectrolyte chain onto a sphere which is given by

$$\frac{12\pi|\sigma q|}{\epsilon b_{\text{eff}} b k_B T}\frac{1-\exp(-2\kappa a)}{\kappa^3} > 1 \qquad (13)$$

where σ is the surface charge density of the sphere, a is the sphere radius, q/b is the linear charge density of the chain, ϵ is the dielectric constant, b_{eff} is an effective Kuhn length of the chain taking into account self-excluded-volume effect and κ is the inverse screening length. The disagreement between our results and Muthukumar's predictions can be explained by the fact that eq 13 is based on enthalpic effects and neglect entropic effects and valid in the limit of large polyelectrolyte chains.

When the polyelectrolyte is adsorbed on the particle surface, its conformation is expected to be different from its conformation in solution. The extent of the change in our simulations is controlled by the polyelectrolyte contour length and C_i. It should be noted that the size ratio between the particle diameter and monomer size is also expected to play a key role but is beyond the scope of this paper. Plots of the ratio of the mean-square radius of gyration $\langle R_g^2\rangle_{ads}$ to the free mean-square radius of gyration $\langle R_g^2\rangle_{free}$ which give a quantitative description of the extent of the change are presented in Figure 4 as a function of C_i. Curves exhibit a nonmonotonic behavior with the chain length N. When $N = 25$, adsorption approaches that on a nearly planar surface. In this case, the chain can fully spread on the surface with dimensions close to its dimensions in a free solution. When chain length is increased up to $N = 140$, polyelectrolytes wrap around the particle to optimize the number of contacts. The conformation of the polymer is then dictated by the particle size and is subject to the highest level of deformation (the maximum is observed when $N = 140$). By increasing further chain length, excluded electrostatic volume prevents any additional monomer adsorption on the surface via the formation of an extented tail in solution. Because of the formation of a protruding tail in solution, the ratio $\langle R_g^2\rangle_{ads}/\langle R_g^2\rangle_{free}$ raises to 1. Owing to the size ratio between the particle diameter and monomer sizes and polyelectrolyte lengths which were investigated in this study, complexes with two tails were not observed during our simulations.

The number of monomers in trains, loops, and tails as a function of N and C_i is presented in parts a and b of Figure 5, respectively, to get insight into the structure of the interfacial region. When the chain length is increased (Figure 5a) with C_i greater than 0.01 M, the total number of monomers in trains and loops increases monotically. When C_i is less than 0.01 M and N greater than 140 monomers, the number of monomers in trains and loops levels off since any additional monomer is expelled in tails. Beyond that critical chain length N^c, intrachain repulsions outweigh the attraction between the monomers and the particle to form tails. It is worth noting here that the length of the tails increases linearly with N above N^c. When short chains are considered, monomers are mainly in trains, whereas a few ones are present in loops. Short chains have thus a tendency to flatten more since this lowers the energy most.

By increasing C_i up to 0.03 M (Figure 5b), the electrostatic excluded volume is decreased, allowing the particle to attract more monomers. Then by increasing further C_i to the critical adsorption/desorption limit C_i^C, the number of monomers in trains decreases while the number of monomers in loops and tails increases to reach a maximum value. When $C_i > C_i^C$, polymer desorption is observed so that the number of monomers in trains, loops, and tails rapidly decreases.

Further insight into the adsorption properties of polyelectrolytes is gained by examining the amount of adsorbed polymer Γ and the particle surface coverage θ. The influence of C_i and N on Γ (Figure 6) clearly demonstrates that the polyelectrolyte ability to be adsorbed on the particle surface decreases with the increase of C_i and N. When $N \geq 140$, Γ reaches a maximum value in the range $0.1\text{ M} > C_i > 0.01$ M, the exact value being dependent on the polyelectrolyte contour length. By increasing further C_i, desorption takes effect and Γ decreases. Variations of surface coverage θ (i.e., the total number of adsorbed monomers in the first layer) as a function of ionic strength and for different degrees of chain polymerization are presented in Figure 7. When $N < N^c$, θ is monotically decreasing with the ionic concentration while a maximum value is

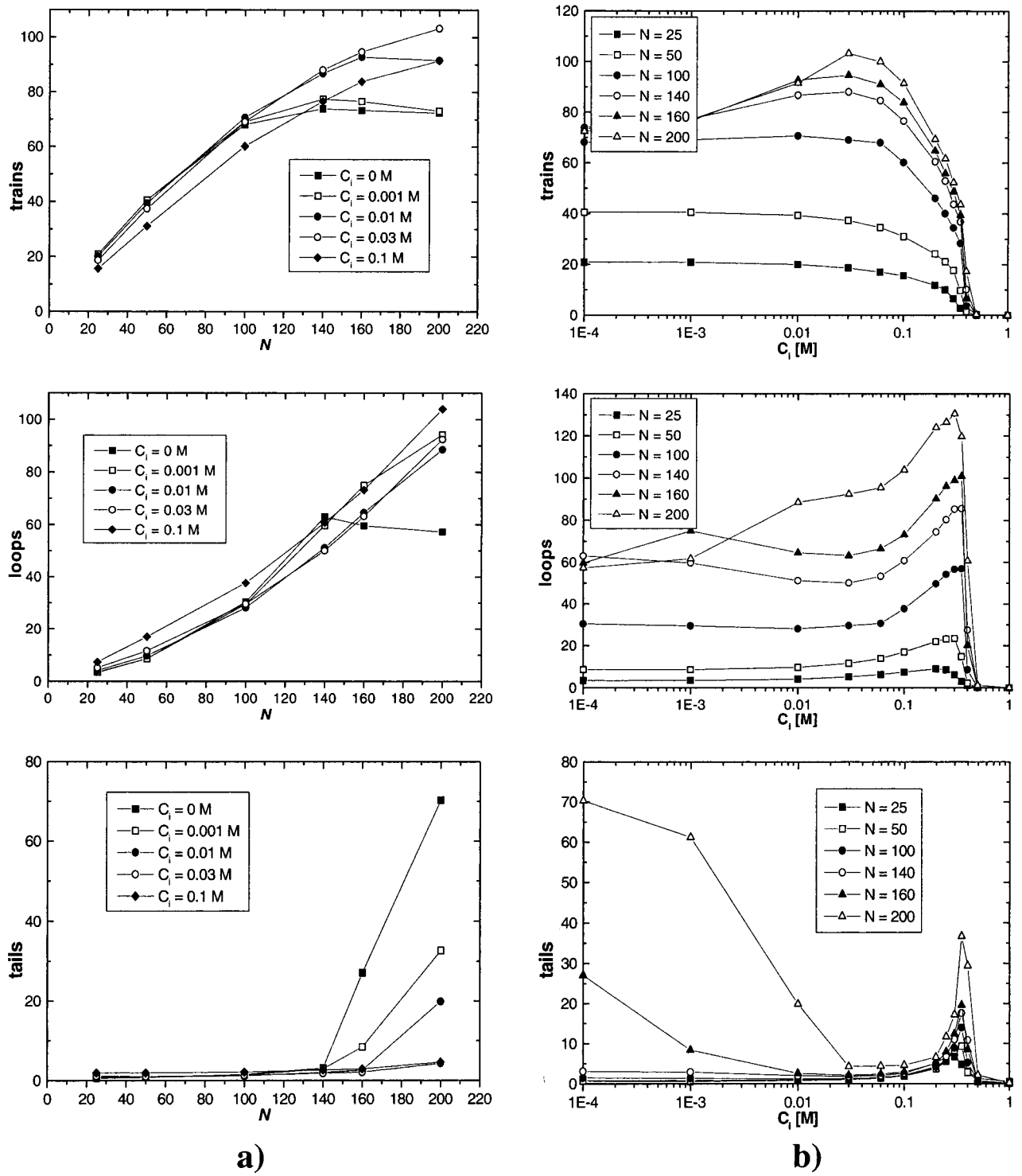

Figure 5. Quantitative description of the interfacial region. Number of monomers in trains, loops, and tails as a function of N and C_i. Because of the formation of a tail in solution and an increase of the capacitance of the particle with C_i, nonmonotonic variations are observed.

achieved when C_i is close to 0.03 M and $N \geq N^c$. These results clearly demonstrate that particle surface coverage and amount of adsorbed polymer are not simple monotonic functions of N and C_i when the polyelectrolyte is large enough to form a tail in solution.

Overcharging. Before starting a discussion with the overcharging issue, some points must first be clarified. Theoretically, collapsed monomers are the ones participating in the overcharging process and are either in contact with the surface of the particle or belong to one of the tightly packed multiple layers. With simulations, this limit is subjective and often fixed arbitrarily owing to the difficulties in deciding where the adsorbed layer ends. In this paper, when overcharging is discussed, the monomers are either adsorbed (N^{ads}) or in tails (N^{tail}), so that the number of adsorbed monomers is defined as $N^{ads} = N - N^{tail}$.

In Figure 8, we plot as a function of N the variation of the number of collapsed monomers N^{ads} in the salt-free case. Our MC simulations and the NS model predictions[35] are presented, and a qualitative and quantitative good agreement is found between the two

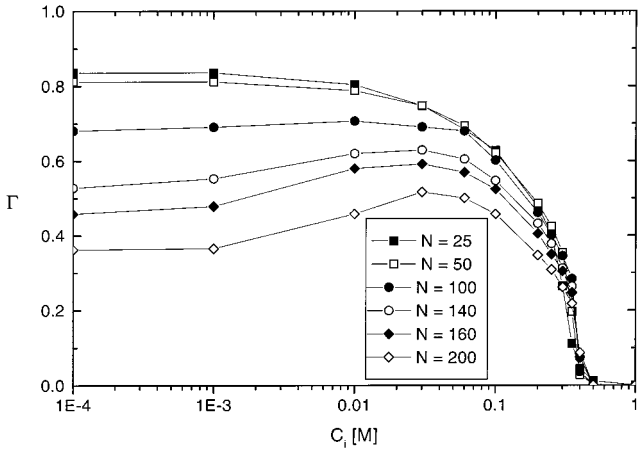

Figure 6. Adsorbed amount Γ of polymer as a function of N and C_i. Data with the coordinates $\log(C_i) = -6$ correspond to the salt-free case.

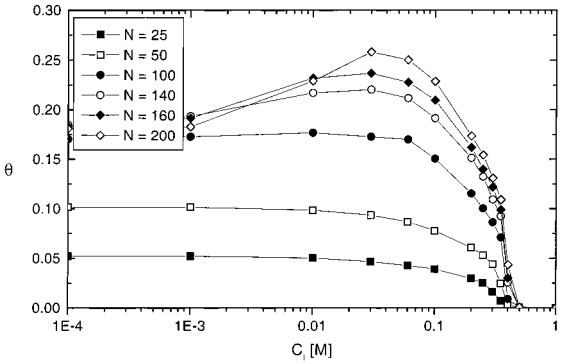

Figure 7. Particle surface coverage θ as a function of N and C_i. Data with the coordinates $\log(C_i) = -6$ correspond to the salt-free case.

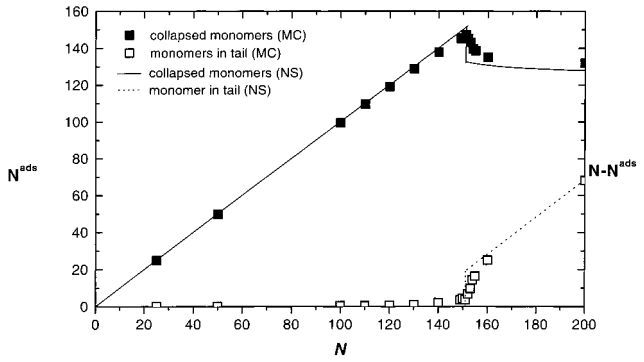

Figure 8. Number of collapsed monomers N^{ads} and monomers in tails ($N - N^{ads}$) as a function of the total number of monomer in the chain N. MC data (squares) are in good agreement with theoretical predictions (lines) of Nguyen and Shklovskii.

models. In a private communication, Nguyen and Shklovskii fitted their equations[35] on our model relating the total free energy of a polyelectrolyte/particle complex to the sum of that spherical complex, the self-energy of the tail, and their interactions. (To find the optimum value of the tail, the total free energy was minimize with respect to the tail length.) A numerical solution giving a first-order transition at $N^c = 151$ with the formation of a protuding tail composed of 19 monomers was obtained in perfect agreement with our observations.

With increasing the size of the polyelectrolyte, several key results are demonstrated: (i) The chain is fully collapsed on the charged particle as long as $N \leq Q$ and $N \approx N^{ads}$, and the complex is undercharged. (ii) When

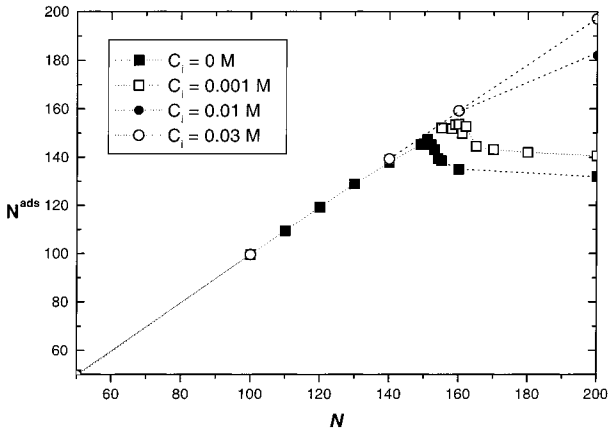

Figure 9. Number of collapsed monomers N^{ads} as a function of the total number of monomers in the chain N, for different values of the ionic concentration. Because of an increase of the particle capacitance N^{ads} increases with C_i.

$N > Q$, more monomers adsorb on the particle surface than is necessary to neutralize it, and the complex is overcharged. Accumulation of monomers close to the surface continues up to $N^c = 151$. (iii) Beyond that critical number of monomers, a protuding tail in solution appears. The NS model[35] predicts a first-order transition at this point followed by a small decrease in N^{ads} with N rapidly reaching a plateau value. Our MC simulations follow this behavior perfectly.

Despite our results supporting the analytical description of complex formation given by Nguyen and Shklovskii, it should be noted that in the NS model the adsorbed part of the chain winds around the macroion to form a solenoid conformation and, as observed in Table 3, such highly ordered conformations are not achieved with our flexible polyelectrolyte model. In our case, the pattern obtained by the collapsed monomers at the particle surface is close to that found on tennis balls. Solenoid-type wrapping is expected to require more locally ordered chains. By including local rigidity, some preliminary results demonstrate that solenoid conformation is achieved. These results will be presented in a future paper.

We now consider the overcharging issue in the presence of added salt. All calculations were performed with $C_i \leq 0.03$ M, i.e., in the adsorption domain, before the desorption process takes place. The number of collapsed monomers as a function of N and C_i is reported in Figure 9. By increasing the screening of the electrostatic interactions, it is clearly demonstrated that the electrostatic volume of the monomers decreases, thus allowing the adsorption of a greater number of monomers on the particle surface. This result supports the NS model which predicts an increase of charge inversion as κ^{-1} decreases. In addition to the increase of charge inversion with C_i, Figure 9 demonstrates that the position of the first-order transition increased with increasing the polyelectrolyte chain length. In particular, when $C_i = 0.01$ and 0.03 M, it is worth noting that a chain composed of 200 monomers is not large enough to induce the formation of a tail.

Conclusions

In the present paper, MC simulations have been used to investigate the adsorption/desorption limit and explore the conformational changes and behavior of a polyelectrolyte in the presence of an oppositely charged

colloidal particle by focusing on the roles of the ionic concentration and monomer number. Adsorption occurs if the loss of entropy of the chain is at least compensated by the gain of energy. Thus, most favorable conditions to achieve adsorption are obtained by considering long chains. Our simulations point out the importance of two competing effects when the ionic concentration increases: on one hand, the particle capacitance increases, and so, much monomers could be adsorbed; on the other hand, the electrostatic attraction between the particle and the monomer becomes less important, giving the monomers and the polyelectrolyte the opportunity to leave the particle surface.

Polyelectrolyte conformational changes resulting from adsorption are found to be dependent on the polyelectrolyte size. Maximum chain deformation is achieved in the low screened limit and when the ratio of the mean end-to-end distance of the free polyelectrolyte to the particle radius is close to 20. By increasing further the chain length, excluded electrostatic volume prevents any additional monomer adsorption on the surface. As a result, an extended tail is formed in solution. Our MC results demonstrate that the complexation between a polyelectrolyte and a charged sphere can lead to overcharging when $N > Q$. We find a perfect agreement with the Nguyen and Shklovskii model both in the salt-free case and in the case of added salt. Variations in the number of adsorbed monomers as a function of the total number of monomers support a first-order transition with the spontaneous formation of a protuding tail in solution.

The simulations reported here are a preliminary step toward a more precise modeling of the problem to get insight into the behavior of more concentrated polymer solutions (systems with several chains) and thus flocculation/stabilization processes of polymer/particle mixtures. A simple model involving one chain interacting with one particle has been described. It will be extended to more complicated systems involving several chains as well as to polydisperse systems. We hope the observations made in this study are particularly useful for choosing an appropriate polymer for applications such as steric stabilization of dispersed particles. We are currently extending our investigations to the adsorption of semiflexible polyelectrolytes.

Acknowledgment. The authors express their thanks to B. Jönsson, B. I. Shklovskii, and T. T. Nguyen for their encouragements and stimulating discussions. We gratefully acknowledge the financial support received from the following sources: Swiss National Research Projects 2000-037589.93/1 and 2000-043568.95/1. The calculations reported here were performed on a DEC 3000-900S. We are also grateful to the University of Geneva for allowing us unlimited use of its Computing Center.

References and Notes

(1) Ledward, D. A. In *Protein Functionality in Food Systems*; Hettiarachchy, N. S., Ziegler, G. R., Eds.; Marcel Dekker: New York, 1994; p 225.
(2) Kendal, K.; Alford, N. McN.; Clegg, W. J.; Birchall, J. D. *Nature* **1989**, *339*, 130.
(3) Napper, D. H. *Polymeric Stabilization of Colloidal Dispersions*; Academic: New York, 1983.
(4) Buffle, J.; Wilkinson, K. J.; Stoll, S.; Filella, M.; Zhang, J. *Environ. Sci. Technol.* **1998**, *32*, 2887.
(5) Strauss, J. K.; Maher, L. J. III *Science* **1994**, *266*, 1829.
(6) Pincus, P. A. In *Lectures on Thermodynamics and Statistical Mechanics*; Gonzalez, A. E., Varea, C., Eds.; XVII Winter Meeting on Statistical Physics; World Scientific: Singapore, 1988; p 74.
(7) Wong, K.; Cabane, C.; Duplessix, R. *J. Colloid Interface Sci.* **1987**, *123*, 466.
(8) Blaakmeer, J.; Böhmer, M. R.; Cohen Stuart, M. A.; Fleer, G. J. *Macromolecules* **1990**, *23*, 2301.
(9) Meadows, J.; Williams, P. A.; Garvey, M. J.; Harrop, R. A.; Phillips, G. O. *Colloids Surf.* **1988**, *32*, 275.
(10) Durand, G.; Lafuma, F.; Audebert, R. *Prog. Colloid Polym. Sci.* **1988**, *266*, 278.
(11) Fleer, G. J.; Stuart Cohen, M. A.; Scheutjens, J. M. H. M.; Cosgrove, T.; Vincent, B. *Polymers at Interfaces*; Chapman and Hall: London, 1993.
(12) Pincus, P. A.; Sandroff, C. J.; Witten, T. A., Jr. *J. Phys. (Paris)* **1984**, *45*, 725.
(13) Muthukumar, M. *J. Chem. Phys.* **1987**, *86*, 7230.
(14) van der Schee, H. A.; Lyklema, J. *J. Phys. Chem.* **1984**, *88*, 6661.
(15) Evers, O. A.; Fleer, G. J.; Scheutjens, J. M. H. M.; Lyklema, J. *J. Colloid Interface Sci.* **1986**, *111*, 446.
(16) Aubouy, M.; Guiselin, O.; Raphaël, E. *Macromolecules* **1996**, *29*, 7261.
(17) Linse, P. *Macromolecules* **1996**, *29*, 326.
(18) Beltrán, S.; Hooper, H. H.; Blanch, H. W.; Prausnitz, J. M. *Macromolecules* **1991**, *24*, 3178.
(19) Böhmer, M. R.; Evers, O. A.; Scheutjens, J. M. H. M. *Macromolecules* **1990**, *23*, 2288.
(20) Granfeldt, M. K.; Jönsson, B.; Woodward, C. E. *J. Phys. Chem.* **1992**, *96*, 10080. Granfeldt, M. K.; Jönsson, B.; Woodward, C. E. *J. Phys. Chem.* **1991**, *95*, 4819. Podgornik, R.; Åkesson, T.; Jönsson, B. *J. Chem. Phys.* **1995**, *102*, 9423. Podgornik, R.; Jönsson, B. *Europhys. Lett.* **1993**, *24*, 501.
(21) Alexander, S. *J. Phys. (Paris)* **1977**, *38*, 977.
(22) McQuigg, D. W.; Kaplan, J. I.; Dubin, P. L. *J. Phys. Chem.* **1992**, *96*, 1973.
(23) Haronska, P.; Vilgis, T. A.; Grottenmüller, R.; Schmidt, M. *Macromol. Theory Simul.* **1998**, *7*, 241.
(24) von Goeler, F.; Muthukumar, M. *J. Chem. Phys.* **1994**, *100*, 7796.
(25) Netz, R. R.; Joanny, J.-F. *Macromolecules* **1999**, *32*, 9026.
(26) Wallin, T.; Linse, P. *Langmuir* **1996**, *12*, 305.
(27) Wallin, T.; Linse, P. *J. Phys. Chem.* **1996**, *100*, 17873.
(28) Wallin, T.; Linse, P. *J. Phys. Chem. B* **1997**, *101*, 5506.
(29) Kong, C. Y.; Muthukumar, M. *J. Chem. Phys.* **1998**, *109*, 1522.
(30) Mateescu, E. M.; Jeppesen, C.; Pincus, P. *Europhys. Lett.* **1999**, *46*, 493.
(31) Wang, Y.; Kimura, K.; Huang, Q.; Dubin, P. L. *Macromolecules* **1999**, *32*, 7128.
(32) Yager, T. D.; McMurray, C. T.; van Holde, K. E. *Biochemistry* **1989**, *28*, 2271.
(33) de Meijere, K.; Brezesinski, G.; Möhwald, H. *Macromolecules* **1997**, *30*, 2337. Caruso, F.; Donath, E.; Möhwald, H. *J. Phys. Chem. B* **1998**, *102*, 2011. Decher, G. *Science* **1997**, *277*, 1232.
(34) Park, S. Y.; Bruinsma, R. F.; Gelbart, W. M. *Europhys. Lett.* **1999**, *46*, 454.
(35) Nguyen, T. T.; Shklovskii, B. I. cond-mat/0005304.
(36) Gurovitch, E.; Sens, P. *Phys. Rev. Lett.* **1999**, *82*, 339. Golestanian, R. *Phys. Rev. Lett.* **1999**, *83*, 2473. Sens, P. *Phys. Rev. Lett.* **1999**, *83*, 2474.
(37) Manning, G. S. *J. Chem. Phys.* **1969**, *51*, 924.
(38) Linse, P. *J. Phys. Chem.* **1986**, *90*, 6821.
(39) Vermeer, R. Interactions between Humic Acid and Hematite and their effects on metal ion speciation. Thesis, Wageningen, 1996.
(40) Allen, M. P.; Tildesley, D. J. *Computer Simulations of Liquids*; Clarendon Press: Oxford, 1987.
(41) Stevens, M. J.; Kremer, K. *J. Chem. Phys.* **1995**, *103*, 1669.

MA000482Z